Thermalization and condensation in an incoherently pumped passive optical cavity

Claire Michel, M. Haelterman, P. Suret, S. Randoux, R. Kaiser, A. Picozzi

Thermalization and condensation in an incoherently pumped passive optical cavity

C. Michel,[1] M. Haelterman,[2] P. Suret,[3] S. Randoux,[3] R. Kaiser,[4] and A. Picozzi[1]
[1]*Laboratoire Interdisciplinaire Carnot de Bourgogne, CNRS, Université de Bourgogne, F-21078 Dijon, France*
[2]*Service OPERA, Université Libre de Bruxelles, B-1050 Brussels, Belgium*
[3]*Laboratoire de Physique des Lasers, Atomes et Molecules, CNRS, Université de Lille, F-59655 Villeneuve d'Ascq, France*
[4]*Institut Non Linéaire de Nice, CNRS, Université de Nice Sophia-Antipolis, F-06560 Valbonne, France*
(Received 1 July 2011; published 26 September 2011)

We study theoretically and numerically the condensation and the thermalization of classical optical waves in an incoherently pumped passive Kerr cavity. We show that the dynamics of the cavity exhibits a turbulent behavior that can be described by the wave turbulence theory. A mean-field kinetic equation is derived, which reveals that, in its high finesse regime, the cavity behaves essentially as a conservative Hamiltonian system. In particular, the intracavity turbulent field is shown to relax adiabatically toward a thermodynamic equilibrium state of energy equipartition. As a consequence of this effect of wave thermalization, the incoherent optical field undergoes a process of condensation, characterized by the spontaneous emergence of a plane wave from the incoherently pumped cavity. The condensation process is an equilibrium phase transition that occurs below a critical value of the (kinetic) energy of the incoherent pump. In spite of the dissipative nature of the cavity dynamics, the condensate fraction of the high-finesse cavity field is found in quantitative agreement with the theory inherited from the purely conservative (Hamiltonian) nonlinear Schrödinger equation.

DOI: 10.1103/PhysRevA.84.033848 PACS number(s): 42.65.Sf, 42.65.Ky, 42.25.Kb

I. INTRODUCTION

The study of the nonlinear evolution of incoherent optical waves is a subject of growing interest in various fields of investigations, including, e.g., wave propagation in homogeneous [1–8] or periodic media [9], nonlinear imaging [10], cavity systems [11–15], or nonlinear interferometry [16]. In particular, the analysis of the long-term evolution of nonlinear incoherent optical waves has been considered in various circumstances [1–3,6,8], as well as in various optical media characterized by different nonlinearities [4,5,7]. When the propagation of the optical wave can be described by a conservative Hamiltonian equation [e.g., NonLinear Schrödinger (NLS) equation], then the evolution of the incoherent wave is characterized by a nonequilibrium process of thermalization [2–4,6,7]. In complete analogy with the kinetics of a gas system, wave thermalization manifests itself by means of an irreversible evolution of the optical field toward the thermodynamic equilibrium state, i.e., the Rayleigh-Jeans equilibrium distribution that realizes the maximum of entropy ("disorder").

The thermalization of the nonlinear wave can be characterized by a self-organization process, in the sense that it is thermodynamically advantageous for the Hamiltonian wave system to generate a large-scale coherent structure in order to reach the most disordered equilibrium state [17]. A remarkable example of this type of self-organization is provided by the condensation of classical nonlinear waves in a defocusing Kerr-like nonlinear medium [18–22]. Nonlinear wave condensation is characterized by the spontaneous formation of a plane-wave starting from an initial incoherent field: The plane-wave solution ("condensate") remains immersed in a sea of small-scale fluctuations ("uncondensed quasiparticles"), which store the information necessary for the reversible evolution of the wave. Wave turbulence (WT) theory [23–25] is known to provide a detailed description of wave condensation, in both the weakly and the highly nonlinear regime of condensation [20,21]. Because this condensation process is a consequence of the natural thermalization of the optical field to thermal equilibrium, it is of a fundamental different nature than the condensation processes recently discussed in optical cavities [11,12,14].

From a different perspective, the thermalization and the Bose-Einstein condensation (BEC) of a photon gas have been recently reported in an optical microcavity [26]. Indeed, in spite of its bosonic nature, the photon gas involved in blackbody radiation does not exhibit a BEC's transition because the number of photons is not conserved due to the interactions of the photon gas with the cavity walls. In the experiments [26], the authors achieve a number-conserving thermalization process by considering a dye-filled optical microresonator, which plays the role of a "white-wall box" for the two-dimensional photon gas. In this way, the authors report an equilibrium BEC's phase transition that results from the thermalization of the photon gas.

Inspired from these recent experiments dealing with the quantum nature of light [26], we study in this paper the condensation and the thermalization of classical optical waves in a Kerr cavity. We consider here a *passive optical cavity* pumped by an incoherent optical wave, whose time correlation, t_c, is much smaller than the round-trip time, $t_c \ll t_R$. In this way, the optical beams from different cycles are mutually incoherent with one another, which makes the optical cavity *nonresonant*. Because of this nonresonant property, the cavity does not exhibit the widely studied dynamics of pattern formation [27,28]. Instead, the dynamics of the cavity exhibits a turbulent behavior that can be characterized by an irreversible process of thermalization toward energy equipartition. We derive a mean-field WT kinetic equation governing the evolution of the averaged spectrum of the incoherent field, which accounts for the incoherent pumping, the nonlinear interaction, and both the cavity losses and propagation losses. In its high-finesse regime, the passive cavity is shown to behave

in a way similar to a conservative system, in the sense that the dynamics of thermalization inherent to the conservative system prevails over the perturbations induced by the external pump and the losses. More specifically, while the initial empty cavity gets filled by the external pump, the intracavity field rapidly relaxes toward a thermal equilibrium state, which is shown to follow adiabatically the slow growth of the intensity in the cavity. As a remarkable result, in its high-finesse regime, the intracavity field undergoes a condensation process below a critical value of the kinetic energy of the incoherent pump, which thus plays the role of the control parameter of the transition to wave condensation. The condensate fraction in the dissipative optical cavity is found in quantitative agreement with the theory inherited from the conservative Hamiltonian NLS equation, without using adjustable parameters.

We underline an important difference that distinguishes the thermalization and condensation processes discussed here with those reported in the quantum context in Refs. [26]. In these latter works, the thermalization process is achieved thanks to an external thermostat—the photons exhibit repeated absorption and re-emission processes in the dye molecules, which thus act as a thermal heat bath reservoir that equilibrates the photon gas to the temperature of the dye molecules. Conversely, in the passive cavity configuration considered here, the process of thermalization solely results from the four-wave interaction mediated by the intracavity Kerr medium (i.e., it results from the nonlinear self-interaction of the optical field), while the "temperature" is controlled by varying the kinetic energy (degree of coherence) of the injected pump.

The study of optical wave thermalization and condensation in a passive cavity offers different important advantages with respect to the free propagation of an optical beam in a nonlinear medium: (i) in the cavity geometry the unavoidable losses due to the propagation in the nonlinear medium do not prevent the system from reaching the stationary thermal equilibrium state; (ii) the dynamics of thermalization can be retrieved experimentally by simply recording the temporal evolution of the field transmitted by the cavity, whereas in the free propagation the analysis of wave thermalization is necessarily limited by the finite length of the nonlinear medium and requires a cutback experimental procedure [3]; (iii) detrimental dissipative nonlinear effects (e.g., Raman scattering) can be filtered out at each round trip. According to these reasons, we believe that this work will stimulate a novel class of experiments aimed at studying new turbulent states of incoherent light in a cavity geometry.

II. MODEL

We are interested in the transverse spatial evolution of an optical beam that circulates in a passive optical cavity containing a nonlinear Kerr medium, whose nonlinear response is assumed to be instantaneous and local for simplicity. Note, however, that this work can easily be extended to a nonlocal nonlinear response or a saturable nonlinearity. In the paraxial approximation, the propagation of the optical beam through the Kerr medium is known to be described by the usual NLS equation [31],

$$i\,\partial_z \psi = -\beta \nabla^2 \psi + \gamma |\psi|^2 \psi - i\alpha\psi, \tag{1}$$

where z ($0 \leqslant z \leqslant L$) denotes the longitudinal spatial coordinate, L being the length of the Kerr medium, and ∇^2 denotes the 2D Laplacian in the transverse plane $\boldsymbol{r} = (x,y)$. γ is the nonlinear Kerr coefficient, α the propagation losses, and $\beta = 1/(2k_0)$ the diffraction coefficient, where k_0 is the wave vector modulus of the optical field in the Kerr medium. It is useful to recall that in the conservative limit ($\alpha \to 0$), the NLS Eq. (1) conserves two important quantities, the intensity of the optical field

$$N = \frac{1}{A}\int |\psi|^2\, d\boldsymbol{r}, \tag{2}$$

where A is the area of integration, and the energy density (Hamiltonian)

$$H = \frac{\beta}{A}\int |\nabla\psi|^2\, d\boldsymbol{r} \; + \frac{\gamma}{2A}\int |\psi|^4\, d\boldsymbol{r}, \tag{3}$$

whose first and second terms, respectively, refer to the linear and nonlinear contributions to the total energy, $H = E + U$. As in the usual studies of wave condensation [18–21], we assume below that the Kerr nonlinearity is defocusing ($\gamma > 0$), so that the plane wave solution (i.e., "condensate state") of the NLS Eq. (1) is modulationally stable. In the following we shall note $\omega(k) = \beta k^2$ the dispersion relation of the linearized NLS Eq. (1), where k refers to the transverse component of the wave vector.

The cavity is pumped by an incoherent optical beam of constant intensity $J_0 = \frac{1}{A}\int |\varphi_m(\boldsymbol{r})|^2 d\boldsymbol{r}$, where $\varphi_m(\boldsymbol{r})$ is the amplitude of the pump field injected at the time $t = mt_R$, where m is the number of round trips. As discussed above, the time correlation of the incoherent pump is much smaller than the round-trip time, $t_c \ll t_R$; i.e., the longitudinal coherence length of the light is much smaller than the cavity length. This means that, in a loose sense, the passive cavity does not behave as a resonant "phase-sensitive interferometer" [29], so that the temporal modes of the cavity do not play any role in the dynamics. In this way, the beam circulating in the cavity and the pump beam are mutually incoherent with each other, and the boundary conditions are not sensitive to the random relative phase among them:

$$\psi_{m+1}(z=0,\boldsymbol{r}) = \sqrt{\rho}\,\psi_m(z=L,\boldsymbol{r}) + \sqrt{\theta}\,\varphi_m(\boldsymbol{r}), \tag{4}$$

where $\psi_m(z,\boldsymbol{r})$ denotes the intracavity optical field after m round trips, with $0 \leqslant z \leqslant L$, while ρ and θ, respectively, refer to the reflection and transmission coefficients of the field intensity, $\rho + \theta = 1$. Note that, for simplicity, we wrote the boundary conditions Eq. (4) with the assumption that the length of the cavity L coincides with the length of the nonlinear Kerr medium. Because the time correlation (t_c) of the pump is much smaller than t_R, the pump beam $\varphi_m(\boldsymbol{r})$ is uncorrelated with itself at each round trip, $\langle \varphi_m(\boldsymbol{r})\,\varphi_p^*(\boldsymbol{r})\rangle = \delta^K_{m,p} J_0$, where J_0 is the average intensity of the pump field and $\delta^K_{m,p}$ denotes the Kronecker symbol. Note that, for the same reason, there is no correlation between the pump and the intracavity field, $\langle \psi_m(z=L,\boldsymbol{r})\,\varphi_m^*(\boldsymbol{r})\rangle \simeq 0$. We also assume that the fluctuations of the incoherent pump are statistically homogeneous in space, i.e., its spatial spectrum is characterized by uncorrelated random spectral phases and the average pump intensity J_0 does not depend on $\boldsymbol{r}$. Besides the time correlation t_c, the incoherent pump is characterized by a spatial correlation length

in its transverse surface section, say λ_c. This correlation length determines the amount of kinetic energy E_J in the pump field, a parameter that will be shown to play a key role in wave condensation.

In order to neglect the temporal dynamics of the cavity, we assume the time correlation of the pump field to be large enough to neglect dispersion effects through the propagation in the Kerr medium. Note that this condition is compatible with the nonresonant cavity condition discussed above, $t_c \ll t_R$. For instance, considering a cavity length L in the range of a meter, we typically have t_R in the range $\sim$10 ns. A time correlation t_c typically less than 1 ns would thus make the cavity nonresonant, while chromatic (or modal) dispersion effects in the Kerr material are usually negligible with such large time correlations [31]. Along the same line, we also assume that the Kerr medium exhibits an anomalous dispersion at the pump frequency, which guarantees the modulational stability of the 3D monochromatic plane wave.

We note that pattern formation in a cavity longer than the coherence length of the light has been considered in Ref. [32]. However, in these previous works the nonlinear medium was characterized by an inertial photorefractive nonlinearity, whose response time $\tau_{\rm res}$ is much longer than the time correlation of the optical field, t_c. As discussed in Ref. [6], such inertial nonlinearity prevents the thermalization (and thus the condensation) of the incoherent optical wave. To summarize, the process of cavity condensation investigated here requires the following hierarchy of the relevant time scales: $\tau_{\rm res} \ll t_c \ll t_R$.

III. MEAN-FIELD KINETIC EQUATION

In order to get some physical insight into the dynamics of the incoherently pumped passive cavity, we develop in this section some preliminary theoretical considerations based on the WT theory. We shall combine the WT kinetic equation that describes the propagation of the field through the Kerr medium ($0 \leqslant z \leqslant L$) together with the cavity boundary conditions Eq. (4) to derive a mean-field WT kinetic equation.

For most purposes, the kinetic wave theory is essentially based on the "random phase approximation," which assumes that the statistics of the field is approximately Gaussian. This approximation is justified in the weakly nonlinear regime, where linear diffraction effects dominate the nonlinear interaction, i.e., $U/E \ll 1$. The random phase approximation breaks the formal reversibility of the NLS Eq. (1), which leads to an irreversible kinetic equation describing the evolution of the averaged spectrum of the field [23–25], $n_m(z,\boldsymbol{k}_1)\delta(\boldsymbol{k}_1-\boldsymbol{k}_2) = \langle \tilde{\psi}_m(z,\boldsymbol{k}_1)\tilde{\psi}_m^*(z,\boldsymbol{k}_2)\rangle$, where $\tilde{\psi}_m(z,\boldsymbol{k}) = \frac{1}{(2\pi)^2}\int \psi_m(z,\boldsymbol{r})\,\exp(-i\boldsymbol{k}\cdot\boldsymbol{r})\,d\boldsymbol{r}$ is the Fourier transform of $\psi_m(z,\boldsymbol{r})$, and $\langle . \rangle$ denotes an average over the realizations of the pump noise. Let us ignore for the moment the cavity boundary conditions; i.e., we consider the propagation of the optical field through the Kerr medium at the round trip m ($\psi_m(z,\boldsymbol{r}), 0 \leqslant z \leqslant L$). Then the WT equation describing the evolution of the averaged spectrum of the optical field reads

$$\partial_z n_m(z,\boldsymbol{k}) = -2\alpha n_m(z,\boldsymbol{k}) + \mathrm{Coll}[n_m(z,\boldsymbol{k})], \tag{5}$$

where the collision term is

$$\mathrm{Coll}[n_m(z,\boldsymbol{k})] = 4\pi\gamma^2 \iiint d\boldsymbol{k}_1 d\boldsymbol{k}_2 d\boldsymbol{k}_3\, \mathcal{N}\, \delta\big[\alpha\big(k_1^2+k_3^2 - k_2^2-k^2\big)\big]\,\delta(\boldsymbol{k}_1+\boldsymbol{k}_3-\boldsymbol{k}_2-\boldsymbol{k}), \tag{6}$$

with

$$\mathcal{N} = n_m(z,\boldsymbol{k})n_m(z,\boldsymbol{k}_1)n_m(z,\boldsymbol{k}_2)n_m(z,\boldsymbol{k}_3)\big[n_m^{-1}(z,\boldsymbol{k})+n_m^{-1}(z,\boldsymbol{k}_2) - n_m^{-1}(z,\boldsymbol{k}_1) - n_m^{-1}(z,\boldsymbol{k}_3)\big]. \tag{7}$$

Note that the derivation of the kinetic Eq. (5) is heuristic, in the sense that its derivation implicitly assumes the dissipative effects perturbative with respect to the four-wave mixing effects underlying the collision term Eq. (6) (see Ref. [18] for details). Actually, the collision term has the same structure as the Boltzmann's kinetic equation describing the nonequilibrium evolution of a dilute classical gas. The kinetic Eq. (5) thus exhibits properties analogous to those of the Boltzmann's equation. In particular, in the conservative limit ($\alpha = 0$), Eq. (5) conserves the intensity of the field $N = \int n_m(z,\boldsymbol{k})\,d\boldsymbol{k}$ and the density of kinetic energy $E = \int \omega(k)\,n_m(z,\boldsymbol{k})\,d\boldsymbol{k}$. The irreversible character of Eq. (5) is expressed by a H theorem of entropy growth, $d_z\mathcal{S} \geqslant 0$, where the nonequilibrium entropy reads $\mathcal{S}(z) = \int \ln[n_m(z,\boldsymbol{k})]\,d\boldsymbol{k}$. The equilibrium distribution that realizes the maximum of entropy subject to the constraints of conservation of E and N is obtained by introducing the respective Lagrangian multipliers $1/T$ and $-\mu/T$. The corresponding thermodynamic Rayleigh-Jeans distribution reads

$$n^{\rm eq}(k) = \frac{T}{\beta k^2 - \mu}, \tag{8}$$

where T and μ are, by analogy with thermodynamics, the temperature and the chemical potential of the field at equilibrium. Because the intensity N and the energy E are conserved quantities, we deal here with a microcanonical statistical ensemble. Note, however, that there is a one-to-one correspondence between (T,μ) and (E,N) [20]. The equilibrium spectrum Eq. (8) is a stationary solution of the kinetic Eq. (6); i.e., it vanishes exactly the collision term of the kinetic Eq. (5). Important to note, the tails of the Rayleigh-Jeans distribution verify the property of energy equipartition among the modes: for $|\mu| \ll \beta k^2$, the energy per mode $\epsilon(k) = \omega(k)n^{\rm eq}(k) = T$ is equally distributed among the modes. The phenomenon of nonlinear wave condensation finds its origin in the divergence of the equilibrium distribution (8): as μ tends to zero, the fundamental plane-wave mode $\boldsymbol{k} = 0$ ("condensate") becomes macroscopically populated, to the detriment of the other modes $\boldsymbol{k} \neq 0$ [20,21].

Let us now consider the boundary conditions of the passive cavity. Taking the Fourier transform of Eq. (4) and neglecting the correlations between the intracavity field and the pump field, we have

$$n_{m+1}(z=0,\boldsymbol{k}) = \rho\, n_m(z=L,\boldsymbol{k}) + \theta\, J(\boldsymbol{k}), \tag{9}$$

where the averaged spectrum of the pump field, $J(\boldsymbol{k}_1)\delta(\boldsymbol{k}_1-\boldsymbol{k}_2) = \langle \varphi_m(\boldsymbol{k}_1)\,\varphi_m^*(\boldsymbol{k}_2)\rangle$, is independent of the round trip m. The absence of correlation between the intracavity field and the pump field, $\langle \tilde{\psi}_m(z=L,\boldsymbol{k})\,\tilde{\varphi}_m^*(\boldsymbol{k})\rangle \simeq 0$, is justified by the

assumption $t_c \ll t_R$, which makes the pump field uncorrelated with itself at each round trip, $\langle \tilde{\varphi}_m(\boldsymbol{k})\, \tilde{\varphi}_p^*(\boldsymbol{k})\rangle = 0$ if $m \neq p$.

In order to derive a mean-field kinetic equation, we assume that the *averaged* spectrum of the field, $n_m(z,\boldsymbol{k})$, exhibits a slow variation within a single round trip. We note that, contrary to the usual mean-field approach [27], we do not assume that the field amplitude $\psi_m(z,\boldsymbol{r})$ exhibits a slow variation within a round trip—the individual speckles of $\psi_m(z,\boldsymbol{r})$ can exhibit rapid variations resulting from the incoherent nature of the beam. Actually, the assumption that the averaged spectrum exhibits slow variations is a rather weak assumption, which implies, in particular, $\theta \ll 1$, $\alpha L \ll 1$, and a weak nonlinearity $U/E \ll 1$. Under this assumption, the evolution of the kinetic Eq. (5) can be averaged over a round trip. Introducing the slow time derivative of the averaged spectrum, $\partial_t \tilde{n}(t,\boldsymbol{k}) = [n_{m+1}(z=0,\boldsymbol{k}) - n_m(z=0,\boldsymbol{k})]/t_R$, where $t = mt_R = mL/v_g$, v_g being the group-velocity of the optical field in the Kerr material, we obtain a mean-field kinetic equation:

$$t_R\, \partial_t \tilde{n}(t,\boldsymbol{k}) = L\, \mathrm{Coll}[\tilde{n}(t,\boldsymbol{k})] + \theta\, J(\boldsymbol{k}) - \Gamma\, \tilde{n}(t,\boldsymbol{k}), \quad (10)$$

where $\Gamma = \theta + 2\alpha L$. Note that the parameter Γ is related to the finesse of the cavity, which is usually defined as $\mathcal{F} = 2\pi/\Gamma$. This kinetic equation simply provides an averaged description of the evolution of the wave spectrum under the influence of the various different effects, namely the nonlinear interaction, the incoherent pump, and both the cavity losses and the propagation losses. Note that the kinetic Eq. (10) does not exhibit a H theorem for the nonequilibrium entropy $\mathcal{S}[\tilde{n}]$ because of the presence of the losses θ and Γ.

As discussed above through the usual kinetic Eq. (5), the collision term in Eq. (10) conserves the intensity N and the density of kinetic energy E of the wave. Then, integrating Eq. (10) over $\boldsymbol{k}$, the collision term vanishes, which readily gives the expression of the temporal evolution of the intensity of the intracavity optical field:

$$N(t) = N(0)\exp(-\Gamma t/t_R) + \frac{\theta}{\Gamma} J_0[1 - \exp(-\Gamma t/t_R)], \quad (11)$$

where $J_0 = \int J(\boldsymbol{k}) d\boldsymbol{k}$ is the pump intensity. According to Eq. (11), the time required to fill the cavity, i.e., the injection time, $\tau_{inj} = t_R/\Gamma$, plays an important role and it can also be viewed as the "average life-time that a photon spends in the cavity" ($1/\Gamma$ being the corresponding average number of round trips). Note that Eq. (11) can be obtained directly from the boundary conditions Eq. (4) and the NLS Eq. (1) without making use of the high finesse assumption underlying the derivation of the mean field Eq. (10). Equation (11) reveals that, regardless of its initial value, the intracavity intensity relaxes exponentially toward a stationary value, N^{st}, determined by the pump intensity and the cavity-propagation losses:

$$N^{\mathrm{st}} = \frac{\theta}{\Gamma} J_0. \quad (12)$$

Note that when the propagation losses can be neglected ($\alpha = 0$), then the intracavity field intensity coincides with the pump intensity, $N^{\mathrm{st}} = J_0$. Proceeding in a similar way, the evolution of the kinetic energy reads $E(t) = E(0)\exp(-\Gamma t/t_R) + \frac{\theta}{\Gamma} E_J[1 - \exp(-\Gamma t/t_R)]$, where $E_J = \int \omega(k)\, J(\boldsymbol{k}) d\boldsymbol{k}$ is the kinetic energy of the pump. Accordingly, the energy $E(t)$ relaxes toward the stationary value

$$E^{\mathrm{st}} = \frac{\theta}{\Gamma} E_J. \quad (13)$$

It is important to note that the energy per particle, E_J/J_0, provides a natural measure of the amount of incoherence in the pump field [30]. Then for a fixed value of the pump intensity, J_0, the energy E_J will appear as the control parameter of the condensation process in the cavity.

The kinetic Eq. (10) explicitly shows that the evolution of the spectrum of the intracavity field is ruled by two antagonist effects. On the one hand, the *linear effects* due to the incoherent pumping and to the cavity-propagation losses enforces the spectrum to relax toward the pump spectrum: neglecting the collision term, the analytical solution of Eq. (10) gives $\tilde{n}(t,\boldsymbol{k}) \to \frac{\theta}{\Gamma} J(\boldsymbol{k})$ for $t \gg \tau_{\mathrm{inj}} = t_R/\Gamma$. On the other hand, as discussed above through the conventional WT Eq. (5), the *nonlinear Kerr effect* described by the collision term in Eq. (10) enforces the field to relax toward the Rayleigh-Jeans distribution (8). We shall see in the next section that in its high-finesse regime ($\Gamma \ll 1$), the dynamics of the cavity is dominated by the collision term in Eq. (10), so that the optical field experiences both the processes of thermalization and condensation.

IV. NUMERICAL SIMULATIONS

The simulations of the incoherently pumped passive cavity have been performed by integrating numerically the NLS Eq. (1) for the field $\psi_m(z,\boldsymbol{r})$ from $z = 0$ to $z = L$. Then we calculate the field $\psi_{m+1}(z=0,\boldsymbol{r})$ by applying the boundary conditions given by the cavity map Eq. (4) at each round trip. For convenience, we normalized the problem with respect to the pump intensity J_0, the longitudinal nonlinear length $L_0 = 1/(\gamma J_0)$, the transverse length $\Lambda = \sqrt{\beta L_0}$, and the time $\tau_0 = L_0/v_g$. The dimensionless variables are obtained through the transformations $z/L_0 \to z$; $\boldsymbol{r}/\Lambda_0 \to \boldsymbol{r}$; $\psi/\sqrt{J_0} \to \psi$; $\varphi/\sqrt{J_0} \to \varphi$; $\alpha L_0 \to \alpha$; $L/L_0 \to L$; and $t/\tau_0 \to t = mL/L_0$. In order to accurately study the influence of the passive cavity on the phenomenon of wave condensation, we compare the simulations of the cavity with those commonly realized in the conservative Hamiltonian limit. We thus performed our simulations in the same conditions as those reported previously in [19–21,33]. In particular, the numerical integration of the dissipative NLS Eq. (1) has been realized by using periodic boundary conditions [in the transverse variables $\boldsymbol{r} = (x,y)$], i.e., by expanding the field amplitude $\psi(z,\boldsymbol{r})$ in the usual plane wave basis [19–21,33]. Besides the robustness and the rapidity of this integration scheme, an essential advantage of the plane wave expansion relies on the fact that it permits us to derive explicit analytical expressions for the condensate amplitude in the *strong nonlinear regime of interaction* [20,21]. More physical configurations of optical wave condensation recently investigated in [22] will be discussed later in Sec. V C.

A. Thermalization

We report in Fig. 1 a typical behavior of the dynamics of the incoherently pumped passive cavity. We considered here

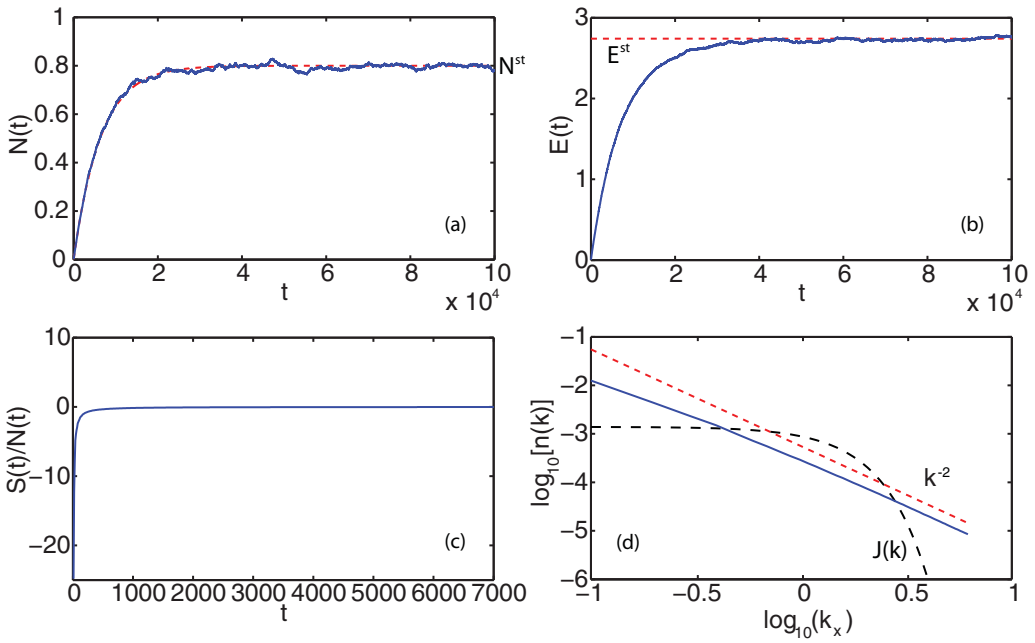

FIG. 1. (Color online) Thermalization: (a) Evolution of the intracavity field intensity N (in units of J_0) vs. time t (in units of mL/L_0) and corresponding temporal evolution of the kinetic energy E (b) and of the "entropy per particle" $\mathcal{S}/N$ (c). The red dashed line in (a) reports the theoretical prediction of the evolution of the intensity given by Eq. (11), the red dashed line in (b) the theoretical stationary value of Eq. (13), $E^{\rm st}$. (d) Averaged spectrum of the field once the cavity dynamics has reached the stationary state (continuous blue line); the tails of the spectrum exhibits an equipartition of energy among the modes, as described by the Rayleigh-Jeans equilibrium distribution Eq. (8); i.e., the power-law $n^{\rm st}(k) \sim k^{-2}$ (red dashed line). The dark dashed line reports the spectrum of the incoherent pump, $J(\boldsymbol{k})$ (characterized by random spectral phases). The parameters are discussed in the text: $A = 64^2\Lambda^2$, 128^2 modes, $L = 8L_0$, $\theta = 0.001$, and $\alpha = 1.5625 \times 10^{-5}L_0^{-1}$ so that $N^{\rm st} = 0.8J_0$.

the natural configuration in which an initial empty cavity, $\psi_{m=0}(z,\boldsymbol{r}) = 0$ for $0 \leqslant z \leqslant L$, is progressively filled by the incoherent pump. The injected pump wave is characterized by a Gaussian-shaped spectrum with random spectral phases—the realizations of the random spectral phases are generated independently of each others, so as to make the incoherent pumps $\varphi_m(\boldsymbol{r})$ uncorrelated at each round trip m. In this example we considered a transverse area of $A = 64^2\Lambda^2$ with 128^2 modes, a cavity length of $L = 8L_0$, and a reflection coefficient of $\theta = 0.001$. The value of the loss parameter $\alpha = 1.5625 \times 10^{-5}L_0^{-1}$ has been chosen in such a way that $N^{\rm st} = 0.8J_0$. Note that the small value of the transmission coefficient considered here can be increased by considering a longer cavity, a feature that will be discussed later in Sec. V B 2. As expected, the cavity exhibits a turbulent behavior, in which the random field amplitude $\psi_m(z,\boldsymbol{r})$ is characterized by statistically homogeneous spatial fluctuations. Because of the high finesse, the pump wave slowly enters into the cavity. As predicted by Eq. (11), the intracavity intensity $N(t)$ relaxes exponentially to the stationary value $N^{\rm st}$ [see Fig. 1(a)]. The kinetic energy E of the field in the cavity follows a similar behavior, as illustrated in Fig. 1(b), which indicates that the optical field reaches a statistical stationary state in the cavity. This is corroborated by the evolution of the entropy "per particle," $\mathcal{S}/N$, which has been normalized to the intensity $N(t)$, so as to compensate for the growth of the "number of particles" in the cavity. Despite the fact that the kinetic Eq. (10) does not exhibit a H theorem, the temporal evolution of $\mathcal{S}/N$ is reminiscent of the usual process of entropy production and saturation encountered in a conservative wave system (see, e.g., [6,21,30]). This is due to the fact the collision term in the kinetic Eq. (10) dominates the dissipative terms related to the cavity and the propagation losses. In particular, the saturation of the process of entropy growth reported in Fig. 1(c) corroborates the fact that the turbulent dynamics of the cavity tends to relax toward a statistical stationary state. We recall in this respect that the entropy, by its definition, is very sensitive to small variations of the tails of the spectrum of the field.

We have analyzed with care the evolution of the spectrum of the field, which has been averaged over the time once the stationary state has been reached, i.e., for $t \gg \tau_{\rm inj} = t_R/\Gamma$. More specifically, we compared an averaging of 1 000 spectra recorded in different time intervals spaced by 10 000 τ_0 ([60 000, 61 000]τ_0, [70 000, 71 000]τ_0, [80 000, 81 000]τ_0, [90 000, 91 000]τ_0, [99 000, 100 000]τ_0), and we did not identify any evolution of the averaged spectrum. We underline that, in the presence of a high finesse, the spectrum of the field relaxes toward a steady state whose tails verify the property of *energy equipartition* among the modes (see Sec. III). This is illustrated in Fig. 1(d), which shows that the tails of the averaged spectrum exhibit the power-law distribution, $n^{\rm st}(k) \sim k^{-2}$, inherent to the thermodynamic equilibrium distribution Eq. (8).

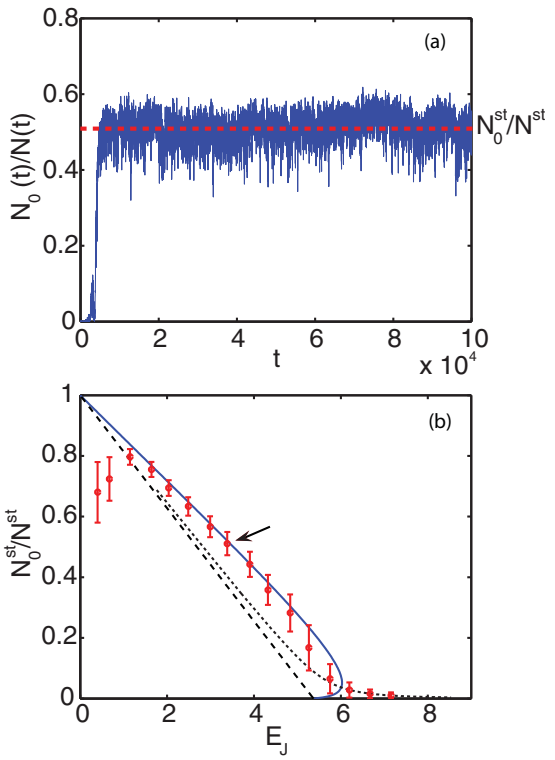

FIG. 2. (Color online) Condensation: (a) Evolution of the fraction of condensed power $N_0(t)/N(t)$ vs. time t (in units of mL/L_0) corresponding to the simulation reported in Fig. 1: the condensate growth saturates to a constant value $N_0^{\rm st}/N^{\rm st}$, which is in agreement with the theory given by Eq. (16) (red dashed line). (b) Condensation curve: fraction of condensed power in the stationary equilibrium state $N_0^{\rm st}/N^{\rm st}$ vs. the kinetic energy of the pump E_J. The condensation curve is computed for a constant value of the pump intensity J_0, while E_J is varied by modifying the degree of coherence of the pump (i.e., its spectral width). The blue solid line is a plot of Eq. (16) and refers to Bogoliubov's regime. The black dotted line is a plot of Eqs. (14),(15) and refers to the WT regime beyond the thermodynamic limit ($\mu \neq 0$), while the dashed black line refers to the thermodynamic limit [$\mu \to 0$ in Eqs. (14) and (15)]. The red points correspond to the numerical simulations of the NLS Eq. (1) with the cavity boundary conditions of Eq. (4). The "error bars" denote the amount of fluctuations in $N_0^{\rm st}/N^{\rm st}$ once the equilibrium state is reached. The arrow in (b) denotes the point corresponding to the simulation reported in (a), $N_0^{\rm st}/N^{\rm st} \simeq 0.51$. Parameters are the same as described in the legend of Fig. 1.

B. Condensation

In the previous paragraph we have shown that, in the presence of a high finesse, the intracavity field exhibits a relaxation toward an equilibrium state that verifies the property of energy equipartition. As a consequence of this thermalization effect, we shall see that the optical field exhibits a condensation process that can be described quantitatively by adapting the theory developed for the purely conservative and Hamiltonian NLS equation [20,21].

We report in Fig. 2(a) the fraction of power, N_0/N, condensed into the fundamental Fourier mode, $\boldsymbol{k} = 0$, as a function of time. This evolution of the condensate amplitude corresponds to the simulation of the cavity discussed in the previous paragraph through Fig. 1. Figure 2(a) shows that the growth of the condensate fraction N_0/N saturates to a constant value during the temporal evolution of the cavity. It is interesting to note that the condensate fraction reaches its asymptotic stationary value [$t \sim 5\,000$ in Fig. 2(a)]*well before* that the cavity reaches its stationary regime [$t \sim 40\,000$ in Fig. 1(a)]. We shall see below in Sec. V A that this is due to the fact that, thanks to the large finesse considered here, the condensate amplitude $N_0(t)$ follows adiabatically the corresponding equilibrium value determined by the instantaneous intensity $N(t)$ of the intracavity field. Let us analyze here the asymptotic condensate amplitude that the field reaches in the stationary regime of the cavity, $N_0^{\rm st}$. Since the passive cavity behaves essentially as a conservative system, we may expect that the stationary value of the condensate amplitude $N_0^{\rm st}/N^{\rm st}$ may be predicted from the theory developed for the conservative (Hamiltonian) problem. We shall now adapt the Hamiltonian condensation theory to the dissipative cavity problem considered here. We anticipate that, as illustrated in Fig. 2(b), a good agreement is obtained between the theory and the cavity simulations without using adjustable parameters.

A rather complete overview on nonlinear wave condensation in the framework of the conservative (Hamiltonian) NLS equation has been reported in Ref. [21]. We thus refer the reader to this article for a detailed derivation of the equations expressing the condensate fraction N_0/N as a function of the energy H—the so-called "condensation curve." In the cavity problem discussed here, the essential difference with respect to the conservative (Hamiltonian) problem is that the intensity ("particle density") $N(t)$ and the energy $H(t)$ are not conserved quantities (see Fig. 1). However, as discussed above, in the high finesse regime the cavity behaves as a conservative system, so that the condensation theory of Ref. [21] can be considered into the stationary regime. There is another important aspect to note. *Contrary to the conservative NLS equation, where the conserved Hamiltonian plays the role of the control parameter in the condensation curve, in the cavity configuration considered here the natural control parameter is the energy of the pump field.* Below we shall thus express the condensate fraction as a function of the kinetic energy of the pump, E_J, and the cavity-propagation losses (α,θ). The condensate amplitude at equilibrium is calculated by following two different approaches.

1. *Wave turbulence regime*

In the presence of a pump characterized by a poor coherence (i.e., a high kinetic energy E_J), the condensate fraction $N_0^{\rm st}/N^{\rm st}$ is weak, and the dynamics are well described by the WT theory, $U/E \ll 1$. In this case, the theory of wave condensation can be applied straightforwardly by simply replacing the values of the intensity and condensate amplitude by the corresponding values in the stationary regime of the cavity, $N \to N^{\rm st}$ and $N_0 \to N_0^{\rm st}$. Introducing furthermore the kinetic energy of the pump from Eq. (13), one obtains

$$E_J(\mu) = \left(J_0 - \frac{\Gamma N_0^{\rm st}}{\theta}\right) \frac{\sum_{\boldsymbol{k}}' \frac{\beta k^2}{\beta k^2 - \mu}}{\sum_{\boldsymbol{k}}' \frac{1}{\beta k^2 - \mu}}, \tag{14}$$

$$\frac{N_0^{\rm st}(\mu)}{N^{\rm st}} = \frac{1}{-\mu} \frac{1}{\sum_{\boldsymbol{k}} \frac{1}{\beta k^2 - \mu}}, \tag{15}$$

where $\sum_{\boldsymbol{k}}'$ denotes a sum over all modes $\boldsymbol{k}$, except the fundamental one $\boldsymbol{k} = 0$. In this expression, finite size effects of the system are taken into account through the nonvanishing chemical potential, $-\mu > 0$. Indeed, in analogy with quantum Bose-Einstein condensation, classical wave condensation occurs beyond the thermodynamic limit in two spatial dimensions, i.e., condensation is reestablished thanks to finite size effects. These aspects have been discussed in detail in Refs. [6,21]. The fraction of condensed particles N_0/N versus the energy of the pump E_J is obtained by means of a parametric plot of Eqs. (14) and (15), and the corresponding condensation curve is reported in Fig. 2(a) (dotted line). In particular, in the thermodynamic limit ($\mu \to 0$), the condensation curve reduces to a straight line [dashed line in Fig. 2(a)], $E_J = (J_0 - \Gamma N_0^{\rm st}/\theta)/Q$, where $Q = \sum' \beta^{-1}k^{-2}/(M-1)$ and M is the number of modes. It becomes apparent that a nonvanishing chemical potential introduces a tail in the condensation curve, which progressively approaches the straight line as the system size (A) increases [6,21]. The thermodynamic limit thus allows us to define a critical value of the pump energy, below which the cavity system undergoes wave condensation, $E_J^c = J_0/Q$.

2. *Bogoliubov's regime*

As the coherence of the pump field is increased (i.e., the kinetic energy E_J decreases), the condensate amplitude becomes strong, so that the dynamics enter into the nonlinear regime of interaction that invalidates the WT theory (the condition $U/E \ll 1$ is no longer verified). Actually, the existence of the plane wave changes the nature of the interaction and Bogoliubov's regime is established: the dynamics turn out to be dominated by the three-wave interaction instead of the four-wave interaction [18]. In this regime, one can still derive a closed relation between the condensate amplitude and the energy into the Bogoliubov basis [20,21]. However, caution should be exercised when applying the procedure of Refs. [20,21] to the cavity configuration considered here. Let us briefly discuss this aspect.

The total Hamiltonian $H^{\rm st} = H_2^{\rm st} + H_R^{\rm st}$ has a second-order contribution ($H_2^{\rm st}$) that comes from the linearization of the NLS equation around the plane wave solution and a remainder contribution $H_R^{\rm st}$. The fluctuations surrounding the condensate plane wave evolve according to the Bogoliubov dispersion relation, $\omega_B(k) = \sqrt{\beta^2k^4 + 2\beta\gamma N_0^{\rm st}k^2}$. Making use of Bogoliubov's transformation, the contribution $H_2^{\rm st} = E^{\rm st} + U_2^{\rm st}$ is diagonalized in Bogoliubov's basis b_k, $H_2^{\rm st} = \sum_{\boldsymbol{k}} \omega_B(k)\langle|b_k|^2\rangle$, where at equilibrium $\langle|b_k|^2\rangle = T/\omega_B(k)$. In the same way, the "noncondensed particles" can be expressed into Bogoliubov's basis, $N^{\rm st} - N_0^{\rm st} = T\sum_{\boldsymbol{k}}'[(\beta k^2 + \gamma N_0^{\rm st})/\omega_B^2(k)]$ [20]. Eliminating the temperature T from these two expressions thus yields $H_2^{\rm st} = (N^{\rm st} - N_0^{\rm st})(M-1)/\sum_{\boldsymbol{k}}[(\beta k^2 + \gamma N_0^{\rm st})/\omega_B^2(k)]$. On the other hand, the remainder contribution to the Hamiltonian, $H_R^{\rm st} = U^{\rm st} - U_2^{\rm st}$, can be calculated from the WT approach, yielding $\langle U^{\rm st}\rangle = \gamma(N^{\rm st\,2} - N_0^{\rm st\,2}/2)$ and $\langle U_2^{\rm st}\rangle = \gamma N_0^{\rm st}(N^{\rm st} - N_0^{\rm st})$. In this way, the condensation curve relating the linear energy $E^{\rm st}$ to the condensate amplitude $N_0^{\rm st}$, reads $E^{\rm st} = -\langle U_2^{\rm st}\rangle + H_2^{\rm st}$. This equation can be expressed in terms of the kinetic energy of the pump E_J and of the losses (θ,α) in the following form

$$E_J = -\gamma N_0^{\rm st}\left(J_0 - \frac{\Gamma N_0^{\rm st}}{\theta}\right) + \left(J_0 - \frac{\Gamma N_0^{\rm st}}{\theta}\right) \times \frac{M-1}{\sum_{\boldsymbol{k}}' \frac{\beta k^2 + \gamma N_0^{\rm st}}{\beta^2k^4 + 2\beta\gamma N_0^{\rm st}k^2}}. \tag{16}$$

The condensation curve Eq. (16) is plotted in Fig. 2(b) (blue line). Its validity is in principle restricted to the strong condensation regime, and, in particular, the hystheresis predicted at the transition to condensation $E_J \sim E_J^c$ is not physical [21]. Indeed, for a small condensate amplitude, the transition to wave condensation is continuous, as described by the WT theory discussed above through Eqs. (14) and (15).

V. DISCUSSION

A. Adiabatic condensation

In Fig. 2(b) we compare the theoretical condensation curves in the weak [Eqs. (14) and (15)] and strong [Eq. (16)] condensation regimes with the numerical simulations of the passive cavity. The "error bars" denote the amount of fluctuations (variances) of the condensate fraction $N_0^{\rm st}(t)/N^{\rm st}(t)$ once the stationary state is reached in the cavity. We note that in the very high condensation regime ($E_J < 1$) there exists some significant discrepancy between the theory and the simulations, a feature that will be discussed in the next paragraph (Sec. V B 1). Besides such high condensation regime, we note that the theory is in quantitative agreement with the simulations of the cavity, without using any adjustable parameter. This good agreement stems from the fact that we considered a cavity characterized by a large finesse, $\mathcal{F} > 10^3$. As mentioned above in Sec. IV B, thanks to such a large finesse, the intracavity field reaches thermal equilibrium before the cavity reaches its stationary regime, i.e., the time required to achieve thermalization, say $\tau_{\rm th}$, is smaller than the injection time, $\tau_{\rm inj} = t_R/\Gamma$ [see Eq. (11)]. In this way, the variations of the intensity $N(t)$ and of the energy $E(t)$ in the cavity are very slow as compared to the thermalization process, so that the equilibrium state of the intracavity field follows adiabatically the slow growths of $N(t)$ and $E(t)$.

It is interesting to note in Fig. 2(a) that the condensate fraction rapidly reaches its asymptotic equilibrium value $N_0^{\rm st}/N^{\rm st}$, and subsequently keeps such a constant value in spite of the slow growths of $N(t)$ and of $E(t)$. This is a consequence of the fact that the intracavity field is permanently at equilibrium during the adiabatic condensation process. This aspect becomes apparent through the analysis of the WT condensation curve Eqs. (14) and (15). Indeed, in the thermodynamic limit ($\mu \to 0$), the fraction of condensed power takes the following simple expression, $N_0/N = 1 - QE(t)/N(t)$. Recalling that the intensity and the energy evolve according to $N(t) = N^{\rm st}[1 - \exp(-\Gamma t/t_R)]$ and $E(t) = E^{\rm st}[1 - \exp(-\Gamma t/t_R)]$ (see Sec. III), then it becomes apparent that the condensate fraction does not depend on time, $N_0/N = {\rm const}$, simply because the ratio $E(t)/N(t) = E^{\rm st}/N^{\rm st}$ remains constant. The same conclusion is obtained from an inspection of the condensation curve in Bogoliubov's regime.

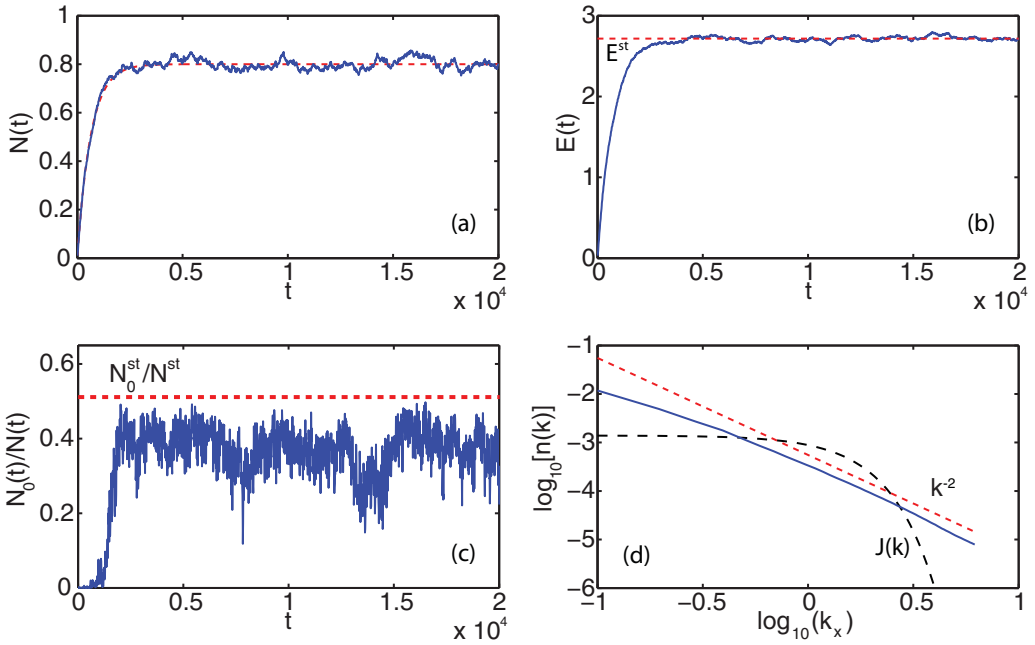

FIG. 3. (Color online) Partial condensation and thermalization: Simulation of the same configuration of the cavity considered in Figs. 1 and 2, except that the transmission coefficient is $\theta = 0.01$. (a) Evolution of the intracavity field intensity N vs. time t (in units of mL/L_0), and corresponding temporal evolution of the kinetic energy E (b). The red dashed line in (a) reports the theoretical prediction of the evolution of the intensity given by Eq. (11), the red dashed line in (b) the theoretical stationary value of Eq. (13). (c) Temporal evolution of the condensate fraction $N_0(t)/N(t)$ (solid blue line) and corresponding theoretical value predicted by Eq. (16) (red dashed line). (d) Averaged spectrum of the field once the cavity dynamics has reached the stationary state (solid blue line). The red dashed line reports the Rayleigh-Jeans Eq. (8) power-law $n^{\rm st}(k) \sim k^{-2}$. The dark dashed line reports the spectrum of the incoherent pump, $J(\boldsymbol{k})$ (characterized by random spectral phases).

The analysis of Eq. (16) reveals that, except for small values of N for which the Bogoliubov approach is not justified, the condensate fraction N_0/N does not depend on the variations of the intensity [i.e., $N(t)$] if the ratio $E(t)/N(t)$ is kept constant. This result may be interpreted intuitively by recalling that the "energy per particle" E/N provides a natural measure of the amount of incoherence in a random wave [30]. In this way, an increase of the number of particles with a constant value of E/N does not lead to a change of the fraction of condensed particles. To summarize, as the cavity gets filled by the incoherent pump, the intracavity optical field rapidly relaxes toward a thermal equilibrium state, which thus follows adiabatically the slow growths of the intensity and of the energy in the cavity.

B. Partial condensation and thermalization

1. *Influence of the finesse*

Up to now we have restricted our study to the analysis of the cavity in its high-finesse regime. However, as one may expect, the cavity no longer behave as a conservative system as the finesse decreases. This is illustrated in Fig. 3, which reports the simulation of the same configuration of the cavity considered in Fig. 1, except that the transmission coefficient has been increased to $\theta = 0.01$. We see in Fig. 3 that, while the intensity $N(t)$ and the energy $E(t)$ follow the expected exponential relaxation toward the stationary regime, the condensate fraction $N_0^{\rm st}/N^{\rm st}$ no longer reach the expected theoretical value of $N_0^{\rm st}/N^{\rm st} = 0.51$ [from Eq. (16)], and the tails of the equilibrium spectrum exhibit some appreciable deviations from the k^{-2} Rayleigh-Jeans power law. In other therms, the cavity and propagation losses (α,θ) are no longer negligible with respect to the collision term in the mean-field kinetic Eq. (10). Nevertheless, the dynamics of the cavity still relaxes toward a stationary regime, which is characterized by a nonvanishing value of the condensate amplitude, i.e., the cavity dynamics exhibit a process of partial condensation and partial thermalization.

The analysis of the numerical simulations reveal that the transition from the complete to the partial thermalization typically occurs when the thermalization time inherent to the conservative (Hamiltonian) NLS equation, $\tau_{\rm th}$, becomes of the same order as the average lifetime of a photon in the cavity, $\tau_{\rm inj} = t_R/\Gamma$. In the regime of adiabatic thermalization discussed above, we had $\tau_{\rm th} \ll \tau_{\rm inj}$. Conversely, when $\tau_{\rm inj} \sim \tau_{\rm th}$, the optical field does not spend sufficient time in the cavity to achieve a complete thermalization process. This interpretation of the cavity dynamics also explains the discrepancy between the theory and the simulations observed in Fig. 2(b) in the high condensation regime, i.e., for $E_J < 1$. Indeed, the thermalization time $\tau_{\rm th}$ of the conservative (Hamiltonian) problem, is known to increase in a significant way in the highly condensed regime. For instance, the numerical simulations reveal that $\tau_{\rm th}$ typically increases by a factor $\sim$10 when the equilibrium condensate fraction increases from 50% to 95%. This can be explained by the fact that in the highly condensed regime the energy H is very small, so that the correlation length of the initial field exceeds the system size,

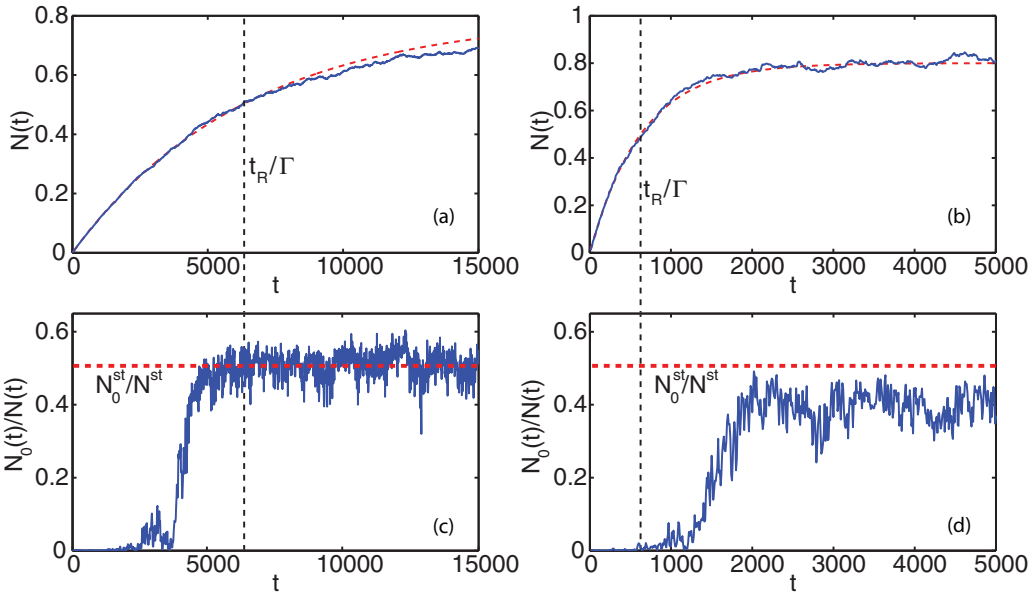

FIG. 4. (Color online) Comparison of the growth time of the condensate fraction $N_0(t)/N(t)$ with the injection time $\tau_{\rm inj}$. (a) and (c), respectively, report a zoom of Figs. 1(a) and 2(a) ($\theta = 0.001$). (b) and (d), respectively, report a zoom of Figs. 3(a) and 3(c) ($\theta = 0.01$). For a high finesse [(a) and (c)], the condensate fraction adiabatically reaches its thermal equilibrium value over a time smaller than $\tau_{\rm inj} = t_R/\Gamma$. As the finesse decreases [(b) and (d)], a partial condensation takes place and the growth of the condensate occurs over a time larger than $\tau_{\rm inj}$.

$\lambda_c > \sqrt{A}$. The time required to reach thermal equilibrium starting from such a highly coherent state is very large: The generation of the new frequency components necessary to reach Bogoliubov's equilibrium state [i.e., energy equipartition $\langle |b_k|^2 \rangle = T/\omega_B(k)$; see Sec. IV B 2] requires a very long transient as compared to the corresponding transient of a highly energetic initial condition verifying $\lambda_c \ll \sqrt{A}$, a feature which is clearly apparent in the simulations. Accordingly, in the high condensation regime of the cavity (small values of E_J), the transient time $\tau_{\rm th}$ becomes larger than the the injection time $\tau_{\rm inj}$, which merely explains the significant discrepancy between the theory and the numerics observed for $E_J < 1$ in Fig. 2(b) [35].

It is interesting to note in Fig. 3 that, although the intracavity field does not reach thermal equilibrium, the growth of the condensate fraction may take place over a time larger than $\tau_{\rm inj}$. This is illustrated in Fig. 4, which compares the injection time $\tau_{\rm inj}$ with the growth-time of the condensate for the two cases analyzed previously through Figs. 2 and 3. Contrary to the adiabatic regime in which the condensate fraction reaches its asymptotic equilibrium value before $\tau_{\rm inj}$ [Figs. 4(a) and 4(c)], in the presence of a lower finesse the growth-time of the condensate becomes larger than $\tau_{\rm inj}$ [Figs. 4(b) and 4(d)]. This indicates that, beyond the simple reasoning that compares $\tau_{\rm inj}$ and $\tau_{\rm th}$, the cavity system has a kind of cumulative memory effect, which allows the intracavity optical field to build the coherent dynamics necessary for the emergence of the condensate.

To complete our study of partial condensation, we report in Fig. 5 the condensation curves for two values of the transmission coefficient higher than that considered in Fig. 2(b). For $\theta = 0.01$ [Fig. 5(a)], we see that, despite the effect of partial condensation, the equilibrium condensate fraction $N_0^{\rm st}/N^{\rm st}$ still grows as the pump energy E_J is decreased. However, at small energies E_J, the condensate fraction saturates for the same reason as that discussed above in Fig. 2(b). The same qualitative behavior is observed as the transmission coefficient increases further [$\theta = 0.04$ in Fig. 5(b)]. However, in this case we may note that the transition to condensation is significantly retarded with respect to the expected critical value E_J^c.

2. *Influence of the cavity length*

We have also considered the influence of the cavity length L on the dynamics of thermalization and condensation. The idea here is to qualitatively assess the influence of the perturbation induced by the pump at each round trip on the coherent state of the condensed optical field. More precisely, we compare the influence of a weak but frequent perturbation, with a strong but rare perturbation of the pump on the condensed field. For this purpose, we vary the length L of the cavity, as well as its transmission coefficient θ, by keeping constant the injection time $\tau_{\rm inj} = t_R/\Gamma = L/[v_g(\theta + \alpha)]$. In this way, we repeat the simulation of Fig. 3, where $L = 8L_0$, for different values of the cavity length, namely $L = 2L_0$ and $L = 32L_0$. The analysis of the numerical results do not reveal any qualitative difference in the dynamics of the cavity or in the stationary value of the condensate fraction N_0/N. This shows that *there exists a large flexibility in the choice of the parameters that define a particular experimental configuration of the passive optical cavity*. For instance, the small value of the transmission coefficient considered in Figs. 1 and 2 (i.e., $\theta = 0.001$), may be increased in a substantial way by simply considering a longer cavity.

C. Waveguide geometry

We recall that the numerical simulations of the NLS Eq. (1) discussed above have been realized with periodic boundary conditions in the transverse variable $\boldsymbol{r}$; i.e., the incoherent wave

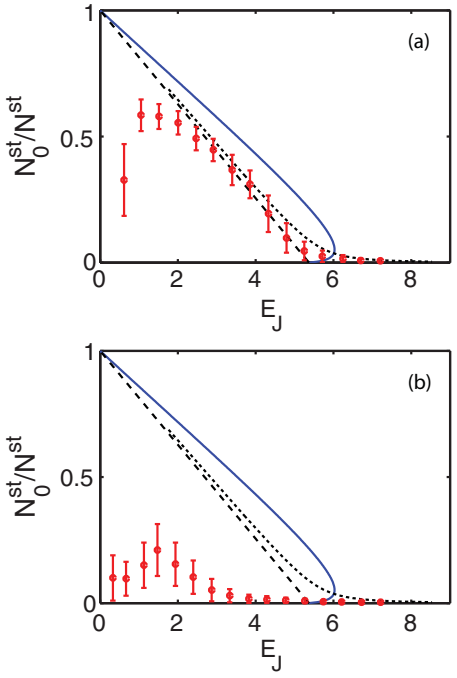

FIG. 5. (Color online) Condensation curves for lower values of the finesse of the cavity, $\theta = 0.01$ (a) and $\theta = 0.04$ (b): fraction of condensed power in the stationary equilibrium state N_0^{st}/N^{st} vs. the kinetic energy of the pump E_J. The blue solid line is a plot of Eq. (16) and refers to Bogoliubov's regime. The black dotted line is a plot of Eqs. (14),(15) and refers to the WT regime beyond the thermodynamic limit ($\mu \neq 0$), while the dashed black line refers to the thermodynamic limit [$\mu \to 0$ in Eqs. (14) and (15)]. The red points correspond to the numerical simulations of the NLS Eq. (1) with the cavity boundary conditions of Eq. (4). The "error bars" denote the amount of fluctuations in N_0^{st}/N^{st} once the stationary regime is reached. Except for the values of the transmission coefficients θ, the parameters are the same as described in the legends of Figs. 1 and 2.

$\psi(z,\boldsymbol{r})$ is expanded in the plane wave Fourier basis. Although this corresponds to the usual numerical approach to study wave condensation [19–21,33], recently, a more realistic physical configuration has been considered in which the incoherent wave propagates in a mutimode optical waveguide [22]. In this case, the optical field is expanded into the eigenmodes of the waveguide and the process of condensation manifests itself through the macroscopic population of the fundamental mode of the waveguide. In particular, it has been shown that the presence of a transverse parabolic index profile (e.g., a graded index multimode optical fiber) reestablishes wave condensation in the thermodynamic limit in two spatial dimensions, in analogy with the genuine quantum BEC [34]. A WT description of the propagation of the incoherent field can still be formulated in this guided wave configuration of the field. The main result is that the collision term in the WT equation involves a fourth-order tensor that accounts for the spatial overlap among the eigenmodes of the waveguide [22]. A qualitative analysis of the kinetic equation revealed that the intricate properties of this new tensor are responsible for a significant slowing down of the thermalization process in the numerical simulations (an accurate determination of a single point in the condensation curve may require several weeks of CPU time). This merely explains why we feel obliged to consider a more flexible numerical approach to explore the dynamics of the incoherently pumped passive cavity. It is clear, however, that the present work of cavity condensation can be extended by performing the NLS simulations in a waveguide configuration. The preliminary work realized in this direction shows that, as one would have expected, the waveguide configuration does not introduce any new qualitative effects into the process of cavity condensation.

VI. CONCLUSION

In summary, we have shown that, in its high finesse regime, an incoherently pumped passive optical Kerr cavity exhibits a turbulent behavior whose properties are analogous to those studied in the framework of the conservative Hamiltonian NLS equation. In particular, in spite of its inherent dissipative nature, the cavity dynamics exhibit a process of adiabatic thermalization, in which the optical field irreversibly relaxes toward the thermodynamic Rayleigh-Jeans equilibrium state. This thermalization process is evidence of several key properties: the growth of the intensity, the energy and the nonequilibrium entropy of the intracavity field, saturate to a stationary value as the system approaches the equilibrium state, while the tails of the stationary spectrum verify the property of energy equipartition. As a consequence of wave thermalization, the intracavity field is shown to exhibit a condensation process, which is an equilibrium transition characterized by the spontaneous emergence of a plane wave from the incoherent field that pumps the cavity. In the high finesse regime, the condensate fraction in the dissipative optical cavity is found in quantitative agreement with the theory inherited from the conservative Hamiltonian NLS equation, except in the very high condensation regime where the transients required to reach equilibrium are particularly long. Conversely, as the finesse decreases, the cavity dynamics relax toward a stationary turbulent regime characterized by a partial condensation and thermalization of the intracavity field. The transition from complete to partial thermalization typically occurs when the thermalization time $\tau_{\rm th}$ becomes larger than the average time that the optical field spends in the cavity, $\tau_{\rm inj}$. We have also seen that the cavity can exhibit a kind of cumulative memory effect, which allows the intracavity field to build its coherent condensed state over a time larger than $\tau_{\rm inj}$.

We finally briefly comment some natural possible extensions of this work. The fact that a statistically stationary steady state of the incoherent field can be sustained in a cavity configuration is an important result that can be exploited to study novel states of incoherent light fields. Besides the condensation and the thermalization processes that result from the analysis of the thermodynamic equilibrium states, the WT theory is known to provide an accurate description of fully developed turbulence in the presence of external sources and sinks that drive the system far from equilibrium [25]. The *nonequilibrium* stationary solutions derived in the framework of the WT theory (i.e., Zakharov-Kolmogorov spectra) play a pivotal role in this framework. So far, in the context of

optics, nonequilibrium stationary solutions have been only investigated in the transient evolution of the system [7], simply because the optical forcing cannot be maintained in the standard configuration in which an optical beam freely propagates through the nonlinear medium. Conversely, in the passive optical cavity discussed here, the optical forcing is nothing but the external pump beam, a remarkable feature that becomes apparent in the mean-field WT kinetic Eq. (10), whose structure is completely analogous to the kinetic equation usually considered to study nonequilibrium stationary solutions in hydrodynamics turbulence [25]. The passive optical cavity then appears as the natural configuration in which the existence of nonequilibrium stationary states of light can be observed and studied in optics.

ACKNOWLEDGMENTS

This work was supported by the Agence Nationale de la Recherche (ANR COSTUME and MANUREVA Projects No. ANR-08-SYSC-004-03 and No. ANR-08-SYSC-019, respectively). The authors thank S. Rica for fruitful discussions.

[1] B. Barviau, S. Randoux, and P. Suret, Opt. Lett. **31**, 1696 (2006); A. Picozzi, *ibid.* **29**, 1653 (2004); A. Picozzi and M. Haelterman, Phys. Rev. Lett. **88**, 083901 (2002); D. V. Dylov and J. W. Fleischer, *ibid.* **100**, 103903 (2008); A. Picozzi, S. Pitois, and G. Millot, *ibid.* **101**, 093901 (2008); A. Fratalocchi, C. Conti, G. Ruocco, and S. Trillo, *ibid.* **101**, 044101 (2008); S. Pitois, A. Picozzi, G. Millot, H. R. Jauslin, and M. Haelterman, Europhys. Lett. **70**, 88 (2005); J. Garnier and A. Picozzi, Phys. Rev. A **81**, 033831 (2010).

[2] A. Picozzi and P. Aschieri, Phys. Rev. E **72**, 046606 (2005); A. Picozzi and M. Haelterman, Phys. Rev. Lett. **92**, 103901 (2004); S. Pitois, S. Lagrange, H. R. Jauslin, and A. Picozzi, *ibid.* **97**, 033902 (2006); B. Barviau, B. Kibler, S. Coen, and A. Picozzi, Opt. Lett. **33**, 2833 (2008); B. Barviau, B. Kibler, and A. Picozzi, Phys. Rev. A **79**, 063840 (2009); A. Picozzi, Opt. Express **16**, 17171 (2008); A. Picozzi, Phys. Rev. Lett. **96**, 013905 (2006); P. Suret, S. Randoux, H. R. Jauslin, and A. Picozzi, *ibid.* **104**, 054101 (2010); C. Michel, P. Suret, S. Randoux, H. R. Jauslin, and A. Picozzi, Opt. Lett. **35**, 2367 (2010); D. B. Soh, J. P. Koplow, S. W. Moore, K. L. Schroder, and W. L. Hsu, Opt. Express **18**, 22393 (2010).

[3] B. Barviau, B. Kibler, A. Kudlinski, A. Mussot, G. Millot, and A. Picozzi, Opt. Express **17**, 7392 (2009).

[4] S. Lagrange, H. R. Jauslin, and A. Picozzi, Europhys. Lett. **79**, 64001 (2007).

[5] L. Levi, T. Schwartz, O. Manela, M. Segev, and H. Buljan, Opt. Express **16**, 7818 (2008)

[6] A. Picozzi, Opt. Express **15**, 9063 (2007).

[7] U. Bortolozzo, J. Laurie, S. Nazarenko, and S. Residori, J. Opt. Soc. Am. B **26**, 2280 (2009).

[8] K. Hammani, B. Kibler, C. Finot, and A. Picozzi, Phys. Lett. A **374**, 3585 (2010).

[9] Y. Silberberg, Y. Lahini, Y. Bromberg, E. Small, and R. Morandotti, Phys. Rev. Lett. **102**, 233904 (2009).

[10] C. Barsi, W. Wan, and J. W. Fleischer, Nature Photon. **3**, 211 (2009).

[11] C. Conti, M. Leonetti, A. Fratalocchi, L. Angelani, and G. Ruocco, Phys. Rev. Lett. **101**, 143901 (2008).

[12] E. G. Turitsyna, G. Falkovich, V. K. Mezentsev, and S. K. Turitsyn, Phys. Rev. A **80**, 031804 (2009).

[13] S. Babin, D. Churkin, A. Ismagulov, S. Kablukov, and E. Podivilov, J. Opt. Soc. Am. B **24**, 1729 (2007); S. A. Babin, V. Karalekas, E. V. Podivilov, V. K. Mezentsev, P. Harper, J. D. Ania-Castan, S. K. Turitsyn, Phys. Rev. A **77**, 033803 (2008); S. Babin, D. V. Churkin, A. E. Ismagulov, S. I. Kablukov, and E. V. Podivilov, Opt. Lett. **33**, 633 (2008).

[14] R. Weill, B. Fischer, and O. Gat, Phys. Rev. Lett. **104**, 173901 (2010); R. Weill, B. Levit, A. Bekker, O. Gat, and B. Fischer, Opt. Express **18**, 16520 (2010).

[15] A. Schwache and F. Mitschke, Phys. Rev. E **55**, 7720 (1997); S. Rutz and F. Mitschke, J. Opt. B: Quantum and Semiclassical Optics **2**, 364 (2000).

[16] Y. Bromberg, Y. Lahini, E. Small, and Y. Silberberg, Nature Photon. **4**, 721 (2010).

[17] V. E. Zakharov *et al.*, Pis'ma Zh. Eksp. Teor. Fiz. **48**, 79 (1988) [JETP Lett. **48**, 83 (1988)].

[18] S. Dyachenko, A. C. Newell, A. Pushkarev, and V. E. Zakharov, Physica D **57**, 96 (1992); Y. Pomeau, *ibid.* **61**, 227 (1992); V. E. Zakharov and S. V. Nazarenko, *ibid.* **201**, 203 (2005).

[19] M. J. Davis, S. A. Morgan, and K. Burnett, Phys. Rev. Lett. **87**, 160402 (2001); Phys. Rev. A **66**, 053618 (2002); P. B. Blakie and M. J. Davis, *ibid.* **72**, 063608 (2005).

[20] C. Connaughton, C. Josserand, A. Picozzi, Y. Pomeau, and S. Rica, Phys. Rev. Lett. **95**, 263901 (2005).

[21] G. Düring, A. Picozzi, and S. Rica, Physica D **238**, 1524 (2009).

[22] P. Aschieri, J. Garnier, C. Michel, V. Doya, and A. Picozzi, Phys. Rev. A **83**, 033838 (2011).

[23] D. J. Benney and P. G. Saffman, Proc. R. Soc. London A **289**, 301 (1966); A. C. Newell, Rev. Geophys. **6**, 1 (1968); A. C. Newell, S. Nazarenko, and L. Biven, Physica D **152**, 520 (2001); Y. Choi, Y. V. Lvov, and S. Nazarenko, *ibid.* **201**, 121 (2005).

[24] V. N. Tsytovich, *Nonlinear Effects in Plasma* (Plenum, New York, 1970); A. Hasegawa, *Plasma Instabilities and Nonlinear Effects* (Springer-Verlag, Berlin, 1975).

[25] V. E. Zakharov, V. S. L'vov, and G. Falkovich, *Kolmogorov Spectra of Turbulence I* (Springer, Berlin, 1992); V. E. Zakharov, F. Dias, and A. Pushkarev, Phys. Rep. **398**, 1 (2004).

[26] J. Klaers, F. Vewinger, and M. Weitz, Nature Phys. **6**, 512 (2010); J. Klaers, J. Schmitt, F. Vewinger, and M. Weitz, Nature (London) **468**, 545 (2010).

[27] L. A. Lugiato and R. Lefever, Phys. Rev. Lett. **58**, 2209 (1987); M. Haelterman, S. Trillo, and S. Wabnitz, Opt. Lett. **17**, 745 (1992).

[28] T. Arecchi, S. Boccalettic, and P. Ramazza, Phys. Rep. **318**, 1 (1999).

[29] S. Coen and M. Haelterman, Phys. Rev. Lett. **79**, 4139 (1997); F. Leo, S. Coen, P. Kockaert, S. P. Gorza, Ph. Emplit and M. Haelterman, Nature Photon. **4**, 471 (2010).

[30] A. Picozzi and S. Rica, Europhys. Lett. **84**, 34004 (2008).

[31] Y. S. Kivshar and G. P. Agrawal, *Optical Solitons: From Fibers to Photonic Crystals* (Academic Press, San Diego, 2003).

[32] T. Carmon, M. Soljacic, and M. Segev, Phys. Rev. Lett. **89**, 183902 (2002); H. Buljan, M. Soljacic, T. Carmon, and M. Segev, Phys. Rev. E **68**, 016616 (2003).

[33] N. G. Berloff, and B. V. Svistunov, Phys. Rev. A **66**, 013603 (2002); N. G. Berloff and A. J. Youd, Phys. Rev. Lett. **99**, 145301 (2007); H. Salman and N. G. Berloff, Physica D **238**, 1482 (2009).

[34] L. Pitaevskii, S. Stringari, *Bose-Einstein Condensation* (Oxford Science Publications, Oxford, 2003).

[35] We have also verified that when the correlation length of the pump becomes larger than the system size, $\lambda_c > \sqrt{A}$, then a significant correlation emerges among different round-trip pumps, $\langle \tilde{\varphi}_m(\boldsymbol{k})\tilde{\varphi}_p^*(\boldsymbol{k})\rangle \neq 0$ for $m \neq p$, a feature that invalidates the derivation of the mean-field kinetic Eq. (10).